INDERSCIENCE PUBLISHERS
Linking academia, business and industry through research

International Journal of Data Mining and Bioinformatics

ISSN online: 1748-5681 - ISSN print: 1748-5673
https://www.inderscience.com/ijdmb

Application of wearable motion tracking devices in training, monitoring, and evaluation

Fangrong Wu, Shuxiang Yang, Chunli Zhang, Huarong Wu

DOI: 10.1504/IJDMB.2026.10077968

Article History:

Received:	17 November 2025
Last revised:	20 January 2026
Accepted:	11 February 2026
Published online:	29 May 2026

Application of wearable motion tracking devices in training, monitoring, and evaluation

Fangrong Wu

College of Physical Education,
Hunan International Economics University,
Changsha, 410205, Hunan, China
Email: 862693656@qq.com

Shuxiang Yang*

School of Nursing and Health Management,
Wuhan Donghu University,
Wuhan, 430212, Hubei, China
Email: ysx_dhxy2024@163.com
*Corresponding author

Chunli Zhang

College of Physical Education,
Hunan International Economics University,
Changsha, 410076, Hunan, China
Email: zhangchunli168268@126.com

Huarong Wu

School of Physical Education,
Changsha University of Science and Technology,
Changsha, 410076, Hunan, China
Email: 9990053@qq.com

Abstract: The current wearable motion tracking devices have significant differences in heart rate monitoring, inaccurate calorie tracking, and measurement errors in exercise speed and distance. Based on this, this paper optimises the design of wearable motion tracking devices. Firstly, this paper establishes a real-time data mining model for sports training wearable devices using fuzzy algorithms, and determines the heterogeneity of sports training data. Then, this paper constructs a feature extraction model and processes the data using thresholding and Savitzky Golay filtering. Subsequently, this paper elaborates on the calibration method of sensors in wearable motion tracking devices, and finally tests the application of the device in training monitoring and evaluation. The research results indicate that the heart rate of student 11 measured by the device in this paper is 84 beats per minute under normal conditions and 123 beats per minute under high-intensity exercise.

Keywords: sports tracking; training monitoring; wearable devices; data processing; device calibration; physiological parameter monitoring.

Reference to this paper should be made as follows: Wu, F., Yang, S., Zhang, C. and Wu, H. (2026) 'Application of wearable motion tracking devices in training, monitoring, and evaluation', *Int. J. Data Mining and Bioinformatics*, Vol. 30, No. 6, pp.71–91.

Biographical notes: Fangrong Wu completed his undergraduate studies at Hunan Institute of Technology and obtained his Master's degree from Hunan Normal University. His research interests include school physical education, physical education, and digitalisation of higher education.

Shuxiang Yang received her Master degree from Wuhan University, P.R. China. Currently, she works in School of Nursing and Health Management, Wuhan Donghu College, Wuhan, 430212, China. Her research interests include biology and health management.

Chunli Zhang studied for both her undergraduate and Master's degrees at the School of Physical Education of Henan University. Her research interests include physical education teaching and sports training.

Huarong Wu completed his undergraduate studies at Wuhan Institute of Physical Education and obtained his Master's degree from Hunan Normal University. His research interests include school physical education, sports humanities and social sciences, and other fields.

1 Introduction

In the digital age, science and technology have a profound impact on human life, especially in sports and health. With improvements in people's living standards and physical fitness, the number of people participating in various sports is also increasing. How to scientifically train and effectively evaluate athletes is currently a concern for people. Wearable motion-tracking tools are a new way to monitor and evaluate sports training (Zhang et al., 2019; Su et al., 2022). By applying advanced technology across disciplines and data analysis, they use motion-tracking devices to measure and record an athlete's movement in real-time, providing coaches and athletes with quantified, objective feedback on their training (Auepanwiriyakul et al., 2020; Bi et al., 2019). For example, in endurance training, coaches can dynamically adjust workout intensity based on real-time observations (via the motion-tracking tool) of their athletes' physiological indicators to avoid overexertion and injuries.

On the other hand, when practicing skills, coaches can independently assess the significant effect of more accurately analysed postural positioning on optimising athletic performance. Nonetheless, there are many limitations of current equipment with respect to consistency across varied and enhanced conditions, variability when moving from one type of motion to another, and discomfort or poor fit due to prolonged use (Zheng and Li, 2024). Without improvements in these technological areas, such equipment will have limited utility and opportunities for more sophisticated and comprehensive training and monitoring/evaluation activities.

This article uses wearable motion tracking devices for training monitoring and evaluation to improve the scientific and practical nature of training. Using this device, accurate recording and analysis of athlete training information can be carried out,

enabling coaches and athletes to understand their training status and effectiveness better and, based on this, develop targeted training plans. This article aims to provide new ideas for health management, personalised fitness, etc. (Wan et al., 2024), through this research, and to promote people's physical health and the healthy development of sports.

Wearable motion-tracking devices (WMTD) can enable real-time monitoring of human movement, which is of great significance for improving health and lifestyle and for advancing related technologies and industries (Manjarres et al., 2019; Liu et al., 2020). In a broad investigation of how inertial measurement units use tracking technology in mobile and sports wearable devices, Song et al. (2021) highlighted the primary issues surrounding motion tracking with these units on said devices and some of the potential solutions to these problems. Liu et al. (2019) used the principles of micro-flow and micro-accelerometry devices to build a human body position tracking system that can be paired with wearable devices for estimating motion from acceleration. A prototype human motion-tracking system for wearable sports devices has been developed by Wilk et al. (2020) designed to track human motion specifically during resistance-strength workouts. Zhou et al. (2022) designed a wearable inertial measurement unit for monitoring three-dimensional finger motion and demonstrated, through experimental validation, that the information obtained with this device type typically yields valid results regardless of sensor positioning, wrist movement, and other factors. It can be seen that many scholars have begun studying WMTD, demonstrating their potential in specific applications, but they also have shortcomings. Scholars have focused more on tracking human posture. However, there are still problems with measuring heart rate and other aspects, which make it difficult for research to meet the needs of training monitoring and require further improvement.

The purpose of reliability research on wearable devices is to ensure the stability of their operational state, optimise the user experience, reduce safety hazards, promote technological development and innovation, enhance industry competitiveness, and support the sustainable development of the industry (Birrer et al., 2014; Nimi et al., 2021). To monitor chewing activity, Hori Kazuhiro has created a small ear-hanging device worn on the lobe that counts the number of times someone chews. The accuracy, precision, and recall of the new chewing-cycle counter were verified by Hori et al. (2021). When researching the reliability of wearable technology, Nickerson et al. (2020) chose athletes as his subjects, examined their performance using a one-way repeated-measures ANOVA, and concluded that all subjects had high intra-class correlation coefficients (ICCs), indicating excellent reliability. Through data analysis, the two research teams noted that they had validated the reliability of wearable technology; however, there remains a need for more research on the accuracy of these technologies when subjected to different environmental conditions and experimental constraints during the research process.

This article provides optimised designs for WMTD for training, assessment, and monitoring. Optimisation occurred through a number of steps, including the collection, processing, and calibration of data from the devices (see section club of the guide). Also, through experimental testing, it was shown that heart rate, calorie expenditure, moving speed, and distance travelled (monitored by the devices in this article) did not vary significantly from the average measurements reported in laboratories. Thus, the accuracy of its monitoring remains strong, providing a reliable means of assessing athletes' training regimens. The key distinguishing factor between this method versus other existing technologies is that the way in which this method has been designed optimises

both the collection and processing of sensor data, which allows for real-time tracking of athlete training data and an increased accuracy in providing a comprehensive view of the evolution of a given athlete's training regimen from start to finish (Wang et al., 2024).

2 Design and optimisation of wearable motion tracking devices

2.1 Data collection

2.1.1 Equipment selection

Training objectives and prerequisites are considered when selecting wearable motion-tracking equipment.

This article uses CC2530 and ADXL345 chips, combined with sensors such as electromyogram (EMG) and resistance, to acquire and convert three-dimensional acceleration and EMG signals, laying the foundation for motion tracking and recognition (Kuchkorov, 2023; Jatakar et al., 2022). Firstly, the ADXL345 accelerometer is used to collect acceleration data in three directions during the athlete's arm movements, and the data is transmitted to the microcontroller through the inter-integrated circuit (IIC) interface for processing before being sent out. Connecting the ADXL345's data and clock lines to one corner of the microcontroller enables the transmission of 3-axial acceleration, EMG, and other electrical signals. Connecting the EMG sensors to the microcontroller via analogue inputs also captures the EMG signal. The parameters for the sensor associated with the selected wearable tracking device can be found in Table 1.

This study also focused on practical application factors, such as energy consumption and the wearable experience, during device optimisation. With regards to energy use, the battery built into the device has enough energy to last about 8 hours when running continuously, meaning that it can be used while continuously monitoring the user's heart rate, acceleration, and sending data; this is enough to carry out a typical training session. Comfort-wise, the device's elastic silicone enclosure weighs only 28 grams. It is ergonomically designed to conform to the curvature of the user's arm. During follow-up interviews, most users reported no sensation of a foreign body or restriction in movement while using the device. Preliminary tests demonstrated that during 1-hour continuous running and strength training sessions, the device did not significantly affect participants' joint range of motion or perceived load. This indicates that the device maintains data accuracy while balancing practical applicability and user experience in real-world training scenarios.

Table 1 Relevant parameters of wearable motion tracking device sensors

Serial number	*Parameter name*	*Parameter value*
1	Processor	ADXL345, CC2530
2	Measure distance	100 metres
3	Scope of work	80 centimetre-40 centimetre
4	Working temperature	-20 degrees Celsius to 70 degrees Celsius
5	Number of valid targets	Ten
6	Camera pixels	In colours, 1.5 million

2.1.2 Node distribution of wearable devices

This article takes WMTD as the research object, uses fuzzy algorithms to obtain real-time data, and establishes a real-time big-data mining model for motion-training wearable devices to measure heterogeneity in real-time motion-training data.

It is assumed that the adjustment voltage, collected from the motion training data of the wearable device, is $\pm U_z$; the resistance load is $V < \phi$; and the boost amplitude, collected from the data, is $U_n = U_z - U_{ED}$. Relevant motion parameters are obtained by placing a large number of sensor nodes during the motion process. During the collection of sports training data, a distributed node combination method for sensor nodes is proposed. Through impedance-adaptive adjustment, the output resonance angle of the sports training data is obtained and represented as γ_0. On this basis, an optimal filter parameter fusion model is established to get the current amplitude A_s, with the initial node's allocation threshold A_O used as the starting point. Real-time motion training data is used as fusion variables, and information parameter $W_{BD} = 0.7$ V of each node is used as input. When collecting sports training data, the terminal current is obtained by adjusting the voltage field on wearable devices. The formula is:

$$A_e = \frac{W_{BD}}{TZ_1 + TZ_2} \tag{1}$$

In the working state of high-frequency switches, this article examines the data output stability of WMTD. It determines the impedance transfer function during motion training. The formula is:

$$\frac{F(z)}{T(z)} = \frac{H_E(z)H_0(z)e^{-\vartheta z}}{1 + H_E(z)H_0(z)} \tag{2}$$

In formula (2),

$F(z)$ data output load of wearable motion tracking devices

$T(z)$ control parameters in distributed sensing data sampling

$e^{-\vartheta z}$ feature parameters connected to the output terminal.

The distribution point set for real-time data collection in sports training can be represented as $Q_j = q_{j1}, q_{j2}, \cdots, q_{jD}$. There is:

$$m \in M_j(g), M_j(g) = \left\{ \left\| a_m(g) - a_j(g) \right\| < t_d(g) \right\} \tag{3}$$

To obtain real-time data of athletes during sports training, a sensor network-based data collection model is constructed (Zhuo et al., 2020; Gao et al., 2020). This model uses association rule scheduling and combines multiple information fusion techniques to accurately capture various types of data during athlete training.

This article uses sensor technology to collect real-time data during the motion training process. It reconstructs the feature quantities of these data using association rules, constructing a model based on fuzzy information fusion to integrate information collected by multiple sensor nodes. Assuming that $a(r)$, $r = 0, 1, \cdots, i - 1$ is the training sequence of real-time data from wearable sports training tracking devices, the state equation for real-time sports training data can be established. On this basis, a discrete fusion processing method is adopted to automatically compile and fuse the motion training data

stored in the database, and a real-time data output feedback adjustment model is constructed to improve the adaptability of the data calculation (Zhang, 2024).

2.1.3 Data collection and output of wearable devices

Using the autocorrelation quantisation fusion tracking analysis method, an adaptive parameter fusion model is constructed for real-time training on motion data. The formula expresses the optimal control state output:

$$\begin{aligned} &\frac{d\varphi}{dr} = \left(\varphi_{\infty}(U) - \varphi\right) \Big/ \delta_N(U) \\ &\varphi_{\infty}(U) = 1 \Big/ \left(1 + e^{-0.1(U+35)}\right) \\ &\delta_N(U) = 400 \Big/ \left(3.3e^{0.05(U+35)} + e^{-0.05(U+35)}\right) \end{aligned} \tag{4}$$

Then, by calculating the impedance characteristic distribution function set B for wearable devices in a collection of sports training data, the devices' impedance outputs are obtained via feedforward control. It is represented as:

$$\left|S_{\varepsilon^G}\varepsilon^G\left(\beta, \delta^*\right)\right| = 1 - |1 - \beta|\, y_0 / C \tag{5}$$

Based on the amplitude information obtained from wearable device data, a feature extraction model for sports training data is constructed by analysing and quantifying real-time amplitude, fusing and tracking identification, and applying it to sports training. Under the conditions of the internet of things (IoT), data collection and fusion processing are carried out on wearable motion tracking devices, and the peak measurement results are as follows:

$$K(\tau, B) = \log \frac{W(\tau, B)}{V(\tau, B)} = \log \frac{\sum_{\delta}^{\delta_{\max}} \left(\tilde{\tilde{b}}_{\delta} - \tilde{b}_{\delta}\right)^2}{\sum_{\delta}^{\delta_{\max}} \left(\tilde{b}_{\delta} - \tilde{b}_{\delta}\right)^2} \tag{6}$$

The transfer function of the data acquisition process for wearable motion tracking devices can be expressed as:

$$\frac{F(z)}{T(z)} = \frac{H_E(z)H_0(z)e^{-\vartheta z}}{1 + H_E(z)H_0(z) - H_n(z)e^{-r}n^z} \tag{7}$$

On this basis, combined with the fuzzy association rule scheduling method, the attribute feature quantities in the data collected during motion training are mined.

Based on the characteristics of sports training data, this article uses a feature-extraction-based motion data processing method, with wearable devices as the research objects, and adds digital circuits on top. Using a binary counter, efficient recording and operation of human body index signals are achieved, and they are displayed and output as time-sharing data packets. To obtain more data, the MAX30100 sensor is used to measure athletes' heart rate and calorie consumption (Hikmah and Indriyanto, 2022; Huang and Guo, 2021). Then, the measured signal is converted to a digital signal and transmitted to the instrument via wireless or wired communication. By processing and analysing digital signals, the spectra and characteristics of signals such as the electrocardiogram (ECG), electroencephalogram (EEG), and EMG can be obtained, thereby enabling evaluation of the body's health status.

Figure 1 Structure of data collection for wearable devices (see online version for colours)

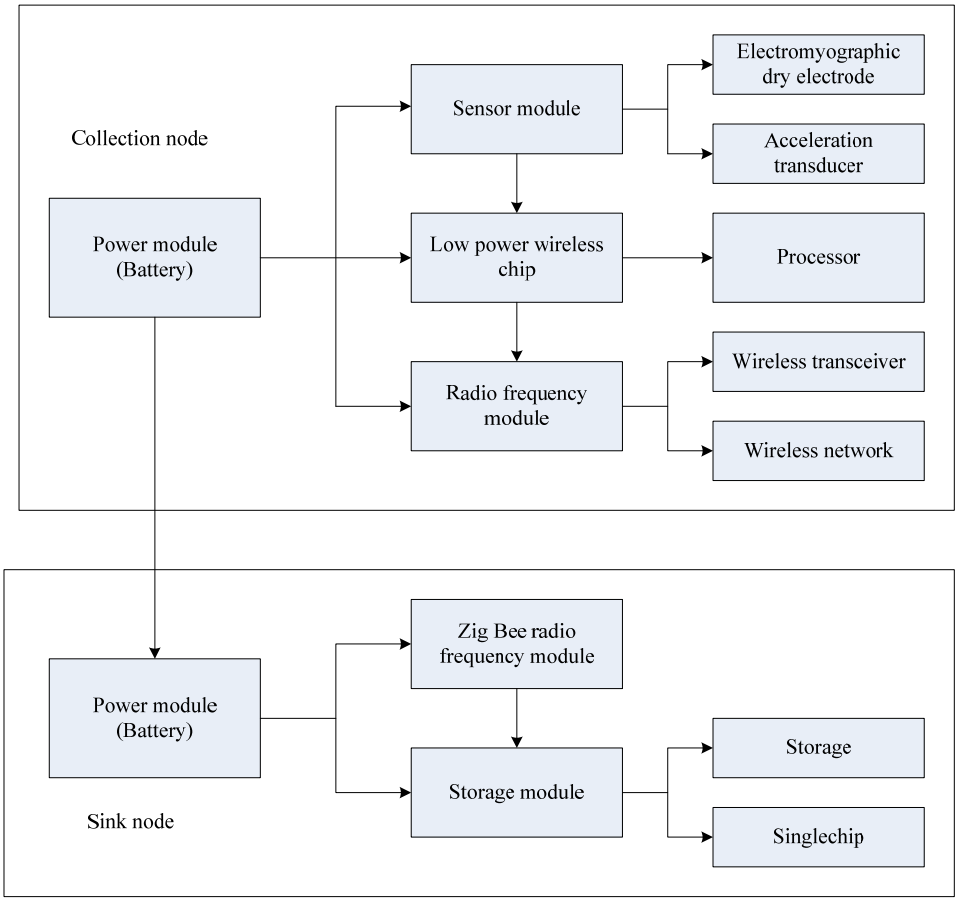

This article aims to use real-time monitoring methods to obtain wearable device data from the l^{th} node in layer *f*. The formula is:

$$\begin{cases} \min_{\beta} \dfrac{1}{2} \sum_{m=1}^{l} \sum_{i=1}^{l} b_m b_i \beta_m \beta_i L(a_m, a_i) - \sum_{i=1}^{l} \beta_i \\ s.t. \sum_{i=1}^{l} b_i \beta_i = 0 \\ 0 \le \beta_i \le v(a_i) E, i = 1, 2, \cdots, l \end{cases} \tag{8}$$

Within the allocation space of the reconstructed action training data, output transformation modulation is applied to the data collected by node ($s\ mm$ = 1, 2, …, M_g). Based on these parameters, a fuzziness-detection model can be developed to collect data from wearable devices for sports training.

After deep processing and the use of correlation graph technology, the core features of sports training data are accurately extracted, and a unique wearable device feature-extraction model is successfully constructed. This model not only enables real-time monitoring and flexible control of data output but also significantly improves the stability

and balance of data collection, providing more accurate and efficient data support for sports training. The data collection structure for wearable devices is shown in Figure 1.

2.2 Data processing

Currently, sensors in WMTD suffer from noise and inconsistent outliers. To reduce noise interference in the data, this article adopts two methods: threshold processing and Savitzky-Golay (SG) filtering (Knight and Bayne, 2019; Schmid et al., 2022).

This article sets three threshold processes: minimum threshold, maximum threshold, and boundary anomaly handling. During the minimum threshold process, when the data is below the set lower limit, it is replaced with the previous value at that point. If expressed in a formula, it is:

$$data\left[data[n] < Min\right] = data[n-1] \tag{9}$$

Among them,

data dataset

$n = 1, \cdots, m$ where n is the index of the dataset, and m is the length of the dataset.

When processing the maximum threshold, if the data is smaller than the set maximum value, the value of the previous non-abnormal sampling point is used as a substitute. The formula is:

$$data\left[data[n] > Max\right] = data[n-1] \tag{10}$$

When the boundary value is abnormal, it is directly excluded.

Multiple strategies have been developed in this research to address communication losses and data-streaming interruptions. The system uses a predetermined threshold and continuously monitors data stream continuity in real-time. If the signal loss exceeds 2 seconds, the system will automatically activate Bluetooth reconnection techniques to restore data transmission. For transient motion-induced anomalies, linear interpolation based on historical data is used to fill gaps. In contrast, sections of data with unusually high values for a sustained period are deemed ‘invalid intervals’. After marking invalid intervals, the system will compute a moving average across valid adjacent points to assess the damage caused by the invalid point. The experiments involve using all devices with built-in local buffers, enabling the safe transfer of data even when communication is lost. When the signal is restored, the data from that experiment automatically synchronises to the analysis terminal to preserve the completeness and accuracy of the dataset.

The following steps are performed under the window so they do not affect subsequent data processing. As an example, the joint angle obtained by sensors is used, and threshold processing is performed in the article; the results are shown in Figure 2. The blue represents raw data, and the red represents processed data. The red box represents the abnormal data.

SG filtering is a digital signal processing technique with a wide range of applications for smoothing and removing noise from data (Rahman et al., 2019; Dombi and Dineva, 2020). The SG filtering method fits the original/raw data with a polynomial and smooths the data (Samann and Schanze, 2019; Sadeghi et al., 2020).

Figure 2 Results before and after threshold processing (see online version for colours)

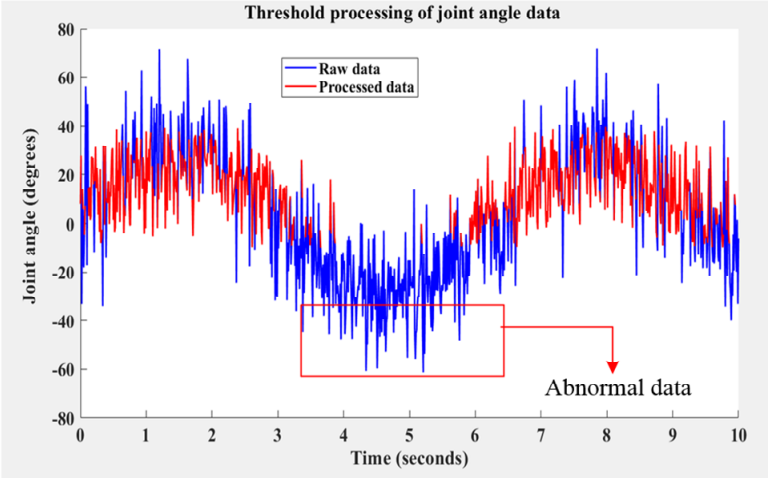

When implementing the SG filtering algorithm, the sliding window size J and the polynomial fitting order (or degree) i are significant parameters that determine its performance (Kagawade and Angadi, 2021; Jiao and Wang, 2021). Generally, an odd number of sliding windows is required, and the polynomial fitting order i should be chosen based on the data's characteristics. The output of the SG filter can be expressed as follows:

$$b_n = \sum_{m=-\frac{1}{2}}^{\frac{J}{2}} [c_m \cdot a_n + m] = c_0 \cdot a_n + c_1 \cdot a_n - 1 + \cdots + c_J / 2 \cdot a_n - \frac{J}{2} \tag{11}$$

In formula (11), $a = [a_1, a_2, a_3, \cdots, a_J]$ is the numerical value of the n^{th} data point in the window. The output is $b_n = [b_1, b_2, b_3, \cdots, b_J]$. J represents the size of the window. c_m represents the m^{th} polynomial fitting coefficient, which can be obtained from formula (12):

$$c_m = \sum_{h=-\frac{J}{2}}^{\frac{J}{2}} y_h \cdot q_m(g / i) \tag{12}$$

Among them, $q_m(a)$ is the j^{th} Legendre polynomial, and y_g is the weight of the g^{th} data point in the window. The calculation formula is:

$$y_g = 1/(\mu^2) \cdot e^{-g^2/(2 \cdot \mu^2)} \tag{13}$$

Among them,

μ the standard deviation of the window

g the corresponding index value in the window.

Figure 3 Sensor data before and after filtering (see online version for colours)

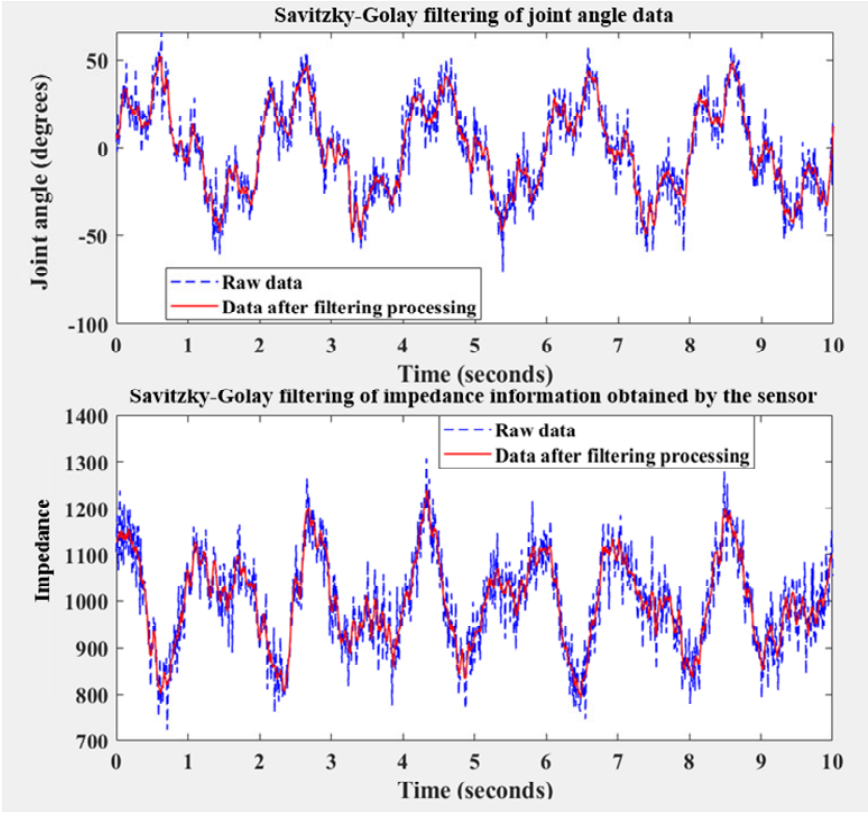

The standard deviation formula can be expressed as:

$$\mu = \sqrt{\frac{\sum_{n}^{J}(a_n - \overline{a})^2}{J-1}} \tag{14}$$

In formula (14), $\overline{a}$ – the average value of all data points in the window.

For example, using joint angle and impedance information from sensors, the SG filter is applied to the data. The specific sensor data before and after filtering is shown in Figure 3.

The first figure in Figure 3 shows the joint angle data obtained by the sensor before and after filtering. The second figure in Figure 3 shows the sensor's impedance before and after filtering. After SG filtering, the data curve is smoother.

2.3 Equipment calibration

The accuracy of WMTD depends on an athlete's training and health. Still, sensor calibration has been recognised as a key technology for the reliable operation of WMTD. The linear displacement sensor (LDS) is an important part of a WMTD, made up of a chip that moves relative to a fixed bracket (Kumar et al., 2019; Yuan et al., 2022). When an external force is applied, the LDS generates a corresponding motion of the chip,

producing linear displacement information related to the target test object. Current methods for calibrating LDSs are problematic due to cumbersome operations, an inability to effectively mitigate measurement inaccuracies between the calibrated object and the reference instrument, and user-involved errors that can reduce the reliability of calibration results. This paper examines the issue of automatic calibration of LDS to mitigate calibration errors, improve the accuracy and efficiency of automatic linear displacement measurement, and thus achieve higher precision during calibration.

The automatic calibration instrument for LDSs mainly comprises a measurement platform, a laser interferometer length-measurement system, a software system, and a measurement driving system. The measurement-driving system precisely controls the position of the test bench, providing a stable environment for laser interferometry measurements. A laser interferometer is a new type of high-precision, high-sensitivity optical interferometer. As the 'brain' of the instrument, the software system can send various instructions to the measurement drive system and summarise and unify these instructions. The main body of the calibration device can be divided into three modules based on their composition: the fixed module for the sensor to be calibrated, the driving module for the sensor's active component, and the main standard module. Its structure is shown in Figure 4.

The fixed module of the sensor to be calibrated can fully meet the installation requirements of various types of LDSs by assembling the cover plate and bottom plate of V-shaped grooves with different structural parameters. At the same time, it is equipped with multi-degree-of-freedom adjustment platforms that can reduce errors caused by tilt and offset during sensor clamping, thereby improving detection accuracy.

The sensor-active-component-driving module is a key component for completing calibration. Among them, the displacement motion platform controlled by the measurement driving system can achieve precise displacement in multiple dimensions, keeping the moving measuring rod of the LDS highly parallel to the laser beam from the laser interferometer.

This investigation used more than just linear-range displacement devices to achieve systematic calibration testing of critical Sensors through a series of tests. An accelerometer (ADXL345) and a heart rate monitor (MAX30100) have been subjected to multi-point static (Calibrated on a standard vibration table) and dynamic (simulated blood flow platform) test methods; these tests assure that the linear error of the Sensors is established for the full operating range at ≤1.5%. Throughout each experiment, each Sensor was calibrated before, during, and following each experiment against thresholds established in accordance with the National 'Sports Sensor Calibration Specification' (GB/T 30106-2013). Calibration data for all critical Sensors were stored in the devices' built-in memory. The data stored in the devices was then automatically compared in real-time against previously established calibration curves using specialised software that provides automated drift alerts. Automated drift alerts and real-time corrections subsequently ensure each Sensor's multi-Sensor data maintains its accuracy for extended periods of use.

The calibration process for sensors in wearable motion tracking devices is as follows. The LDS is installed on the instrument platform, and initial debugging is performed through a precision adjustment device with multiple degrees of freedom. Then, the output end is connected to the digital multifunctional instrument of the power supply and calibration device. Next, all the devices are turned on. After launching the software, the relevant calibration parameters for the LDS are entered. When the laser interferometer's

light source is stable, and the sensor parameters are normal, the software displays the laser interferometer's displacement data and the sensor that needs correction. By activating the calibration function of the displacement sensor via software, the measurement driving system drives the platform to descend, and when the maximum stroke is reached, the platform stops. The calibration data is analysed. If its linearity exceeds the specified limit, it should be located. After the calibration work is complete, it is time to find the zero point. The calibration point parameters and the required number of calibrations are entered to initiate automatic calibration. After automatic calibration completes, the software analyses the calibration results and, upon confirmation of their accuracy, generates the original records. Then the results are output. Finally, calibration is complete, and the software is exited, turning off the power to each device and removing the calibrated LDS from the instrument.

Figure 4 Structure of calibration device (see online version for colours)

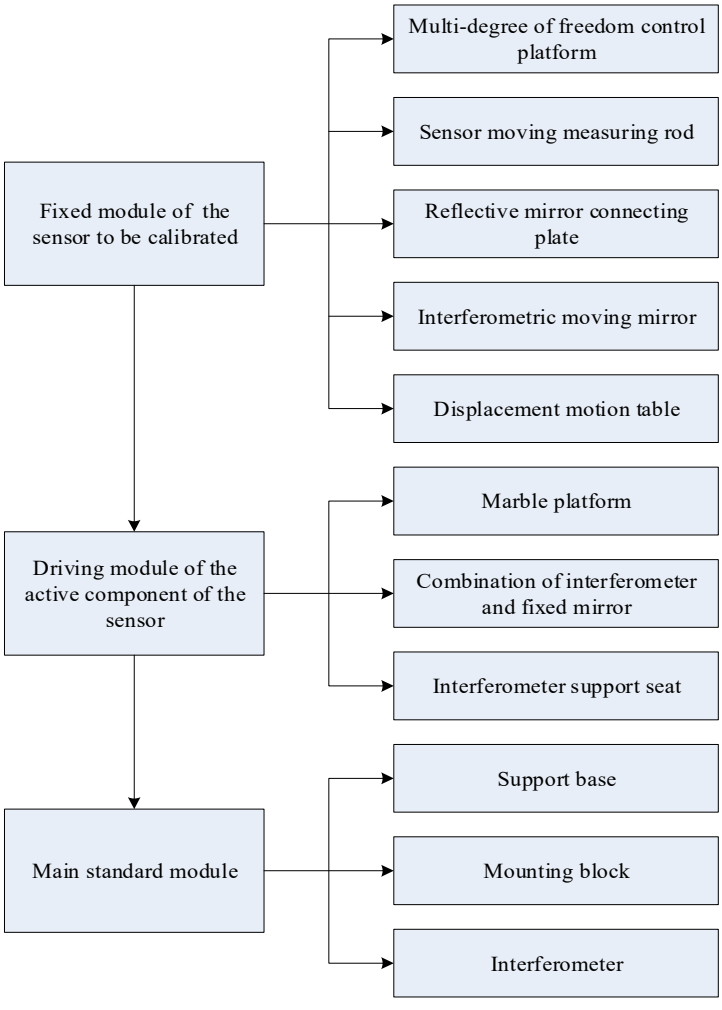

3 Application effect of wearable motion tracking devices in training, monitoring, and evaluation

3.1 Experimental design and data sources

To evaluate the application of the wearable motion-tracking device designed in this article for training monitoring and evaluation, 11 sophomore students from local sports colleges are randomly selected as experimental subjects. Heart rate, calorie consumption, motion speed, and motion distance were collected from 11 male students. The data collected using the device in this article, the device in reference 7, and the device in reference 8, as well as standard data from laboratory testing, are compared to evaluate the device's value for training monitoring and evaluation. The basic information about the 11 selected students is shown in Table 2:

Table 2 Basic information of 11 students

Student serial number	*Age*	*Weight (kg)*	*Height (m)*	*Speciality*
1	19	75.6	1.75	Sports training
2	20	82.4	1.78	Sports training
3	19	84.9	1.81	Physical training
4	19	81.3	1.79	Ethnic traditional sports
5	20	87.7	1.83	Physical training
6	19	74.9	1.75	Ethnic traditional sports
7	21	76.6	1.76	Sports humanities
8	21	86.3	1.82	Physical training
9	20	79.5	1.77	Sports rehabilitation
10	20	88.6	1.85	Sports training
11	20	87.3	1.84	Sports humanities

To ensure experimental rigor and the generalisability of conclusions, this study prioritised sample representativeness and controlled experimental conditions. Eleven second-year students from local sports colleges were randomly selected, covering diverse disciplines including sports training, sports humanities, and ethnic traditional sports. While the sample sizes available for the studies may appear small, the studies extensively used standardised training protocols (e.g., high-intensity exercise, jogging, sprinting) in conjunction with controlled environmental factors (e.g., equipment position) and controlled timing of data collection to reduce external influences. All experimental data were repeatedly validated against laboratory standards and subjected to cross-validation, providing additional evidence to support the data and confirm the internal validity of the collected data. The research results also provided controlled verification of the device's ability to monitor performance during training.

To maintain a consistent environment and reproducible experimental data throughout the study, strict controls were placed upon several environmental variables that may have affected the results. These included controlling the temperature (20 ± 2°C) and humidity (50% ± 5%) within the sports laboratory where all experiments were performed, to eliminate any potential effects of temperature or humidity on perspiration rate and sensor performance, as well as the effect of light on the optical sensors (i.e., MAX30100). In

addition, all floors within the laboratory were constructed from identical material, i.e., professional-grade plastic athletic track surfaces, to ensure no differences could arise from variations in surface materials during testing. Furthermore, testing sessions occurred within a set time frame (9:00 to 11:00 AM) daily to eliminate potential effects from circadian rhythm variations or from diurnal environmental factors that might affect other physiological parameters. Thus, when conducting any form of testing, the results obtained will be more consistent/reliable due to the elimination of variability between test times.

3.2 Experimental results

3.2.1 Monitoring results of heart rate

The ability to measure a student's heart rate in real-time via a wearable Motion-tracking Device is one of the major capabilities of that technology. This type of monitoring allows coaches to see how a student's level of exertion and recovery time fits into their workout routine and to make informed decisions about how to modify a training program to improve a student's safety and overall health. This article will examine heart rate monitoring data collected from a sample of 11 student subjects under both standard and high-intensity exercise conditions, and compare them with corresponding data collected in a laboratory setting. This study defined 'high-intensity exercise' as a standardised intermittent-load test performed on a power bicycle, specifically using a '30-second all-out sprint + 4-minute active recovery' cycle pattern, repeated for 4 sets. The exercise intensity was monitored at 85%–95% of the heart rate reserve to ensure all subjects experienced comparable physiological loads. The results are shown in Figure 5:

Figure 5 Situations of students' heart rate, (A) students' heart rate under normal conditions (B) students' heart rate during high-intensity exercise (see online version for colours)

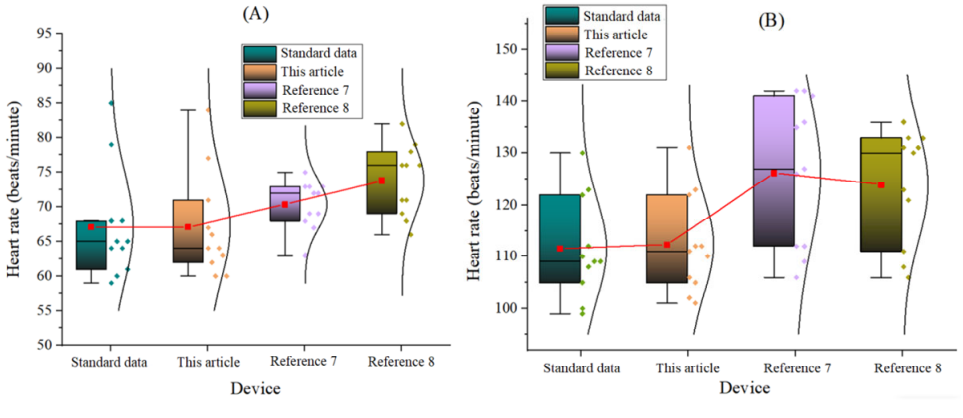

As shown in Figures 5(A) and 5(B), student 1's heart rate is 68 beats per minute under normal conditions and 105 beats per minute during high-intensity exercise. When the device in this article is used for monitoring, the normal heart rate is 67 beats per minute, and the heart rate during high-intensity exercise is 106 beats per minute. When the device in reference seven is used for monitoring, the normal heart rate is 73 beats per minute, and the heart rate during high-intensity exercise is 135 beats per minute. When the device

in reference eight is used for monitoring, the normal heart rate is 69 beats per minute, and the heart rate during high-intensity exercise is 123 beats per minute. Student 11 has a normal heart rate of 85 beats per minute and a heart rate of 123 beats per minute during high-intensity exercise. When the device in this article is used for monitoring, the normal heart rate is 84 beats per minute, and the heart rate during high-intensity exercise is 123 beats per minute. When the device in reference seven is used for monitoring, the normal heart rate is 73 beats per minute, and the heart rate during high-intensity exercise is 136 beats per minute. When the device in reference eight is used for monitoring, the normal heart rate is 76 beats per minute, and the heart rate during high-intensity exercise is 136 beats per minute. It can be seen from these that the monitoring results of the device in this article are closest to the standard data measured in the laboratory, which indicates that the device in this article can more accurately monitor the heart rate of students, accurately reflect their exercise training intensity and physical condition, and better achieve training monitoring.

3.2.2 Monitoring results of calorie consumption

By monitoring calorie intake during exercise, coaches and students can gain an intuitive understanding of energy expenditure and make reasonable adjustments to exercise intensity and strategies. For this purpose, this article collects calorie consumption per hour for 11 students during high-intensity exercise using three devices and compares it with standard laboratory data. The results are shown in Figure 6.

Figure 6 Calorie consumption of 11 students (see online version for colours)

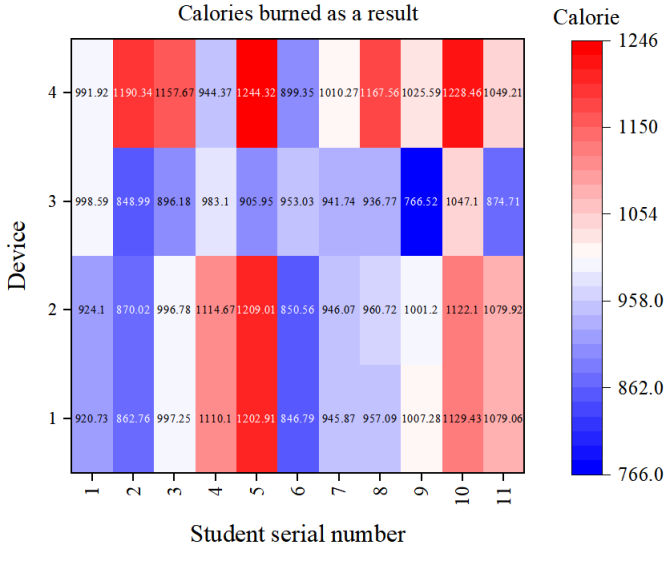

Notes: The 1, 2, 3, and 4 on the vertical axis in Figure 6 represent laboratory standard data, the device in this article, the device in reference 7, and the device in reference 8, respectively. The horizontal axis represents the students' serial numbers.

According to Figure 6, the standard calorie consumption per hour for student one during high-intensity exercise is 920.73; for student 5, 1,202.91; and for student 11, 1,079.06. When the device in this article is used for measurement, the calorie consumption per hour

of student one during high-intensity exercise is 924.10; that of student 5 is 1209.01; that of student 11 is 1,079.92. When the device in reference seven is used for measurement, the calorie consumption per hour for student one during high-intensity exercise is 998.59; that of student 5 is 905.95; and that of student 11 is 874.71. When the device in reference eight is used for measurement, the calorie consumption per hour of student one during high-intensity exercise is 991.92; that of student 5 is 1,244.32; that of student 11 is 1,049.21. Among the measurement results from the three devices, the results obtained with the device in this article are closest to the standard data, indicating that the device's application in sports training monitoring and evaluation is practical.

3.2.3 Monitoring results of motion speed

Accurate speed data can also help coaches analyse athletes' technical characteristics, playing styles, and other factors to deliver targeted training. For this purpose, this article collects the jogging speeds of 11 students during jogging training and compares them with standard data. The specific results are shown in Figure 7.

Figure 7 Motion speed of 11 students during jogging training (see online version for colours)

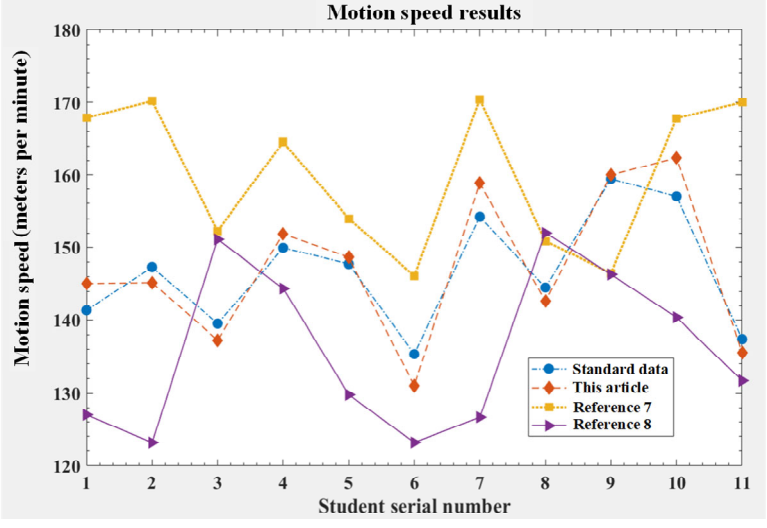

As shown in Figure 7, the motion speed of student one during jogging training measured by the laboratory is 141.34 meters per minute; the motion speed of student five during jogging training is 147.77 metres per minute; the motion speed of student 11 during jogging training is 137.42 metres per minute. When the device in this article is used for monitoring, student 1's jogging training speed is 145.07 metres per minute; student 5's jogging training speed is 148.65 metres per minute; student 11's jogging training speed is 135.56 metres per minute. When the device in reference seven is used for monitoring, student 1's jogging speed is 167.85 metres per minute; student 5's jogging speed is 154.00 metres per minute; student 11's jogging speed is 170.01 metres per minute. When the device in reference eight is used for monitoring, student 1's jogging training speed is 127.01 metres per minute; student 5's jogging training speed is 129.80 metres per minute; student 11's jogging training speed is 131.69 metres per minute. From the above data, it

can be seen that there are significant errors when using the devices in references 7 and 8 for monitoring motion speed. In contrast, the device in this article yields results that are more consistent with standard laboratory data. This indicates that the device described in this article performs better and collects student sports data more accurately, which is beneficial for coaches to analyse their technical characteristics and sports styles better and to provide targeted guidance and training.

In addition to collecting statistics on students' jogging speeds, three WMTD are used to measure their fast-running speeds. The specific results are shown in Table 3.

Table 3 Motion speed of students during fast running training

Student serial number	*Standard data (meters per minute)*	*This article (meters per minute)*	*Reference 7 (meters per minute)*	*Reference 8 (meters per minute)*
1	289.76	290.59	246.87	269.17
2	262.76	263.75	243.78	269.29
3	278.15	279.70	267.92	279.35
4	258.60	253.75	258.22	247.72
5	273.31	271.02	242.33	265.68
6	260.61	259.17	271.09	271.40
7	295.54	293.89	249.14	276.47
8	296.10	299.22	269.86	266.01
9	266.67	263.29	250.31	241.09
10	300.13	298.64	251.01	247.15
11	295.01	296.00	233.83	273.90

According to Table 3, the motion speed of student one during fast running training measured by the laboratory is 289.76 metres per minute; the motion speed of student five during fast running training is 273.31 metres per minute; the motion speed of student 11 during fast running training is 295.01 metres per minute. When the device in this article is used for monitoring, student 1's motion speed during fast running training is 290.59 metres per minute; student 5's motion speed during fast running training is 271.02 metres per minute; student 11's motion speed during fast running training is 296.00 metres per minute. When the device in reference seven is used for monitoring, student 1's motion speed during fast running training is 246.87 metres per minute; student 5's is 242.33 metres per minute; and student 11's is 233.83 metres per minute. When the device in reference eight is used for monitoring, student 1's motion speed during fast running training is 269.17 metres per minute; student 5's is 265.68 metres per minute; and student 11's is 273.90 metres per minute. The data measured by the device in this article are more consistent with the standard laboratory data.

3.2.4 Monitoring results of motion distance

Motion distance monitoring is also an essential indicator for training monitoring and evaluation. Accurate sports distance data can help coaches comprehensively analyse students' physical condition and sports performance, and design more effective training plans and tactics. This article counts the motion distance of 11 students during exercise training and compares it with standard data. The specific results are shown in Figure 8:

Figure 8 Result statistics of motion distance (see online version for colours)

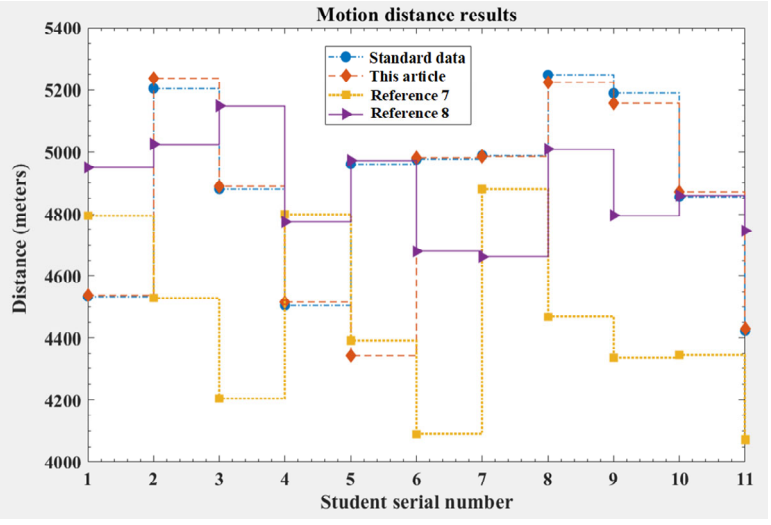

From Figure 8, it can be seen that for student 1, the standard distance data measured during exercise training by the laboratory is 4,533.98 metres; the motion distance measured by the device in this article is 4,537.15 metres; the motion distance measured by the device in reference 7 is 4,795.00 metres; the motion distance measured by the device in reference 8 is 4,950.98 metres. For student 5, the standard data of motion distance measured by the laboratory during training is 4,961.71 metres; the motion distance measured by the device in this article is 4,343.85 metres; the motion distance measured by the device in reference 7 is 4,391.40 metres; the motion distance measured by the device in reference 8 is 4,973.12 metres. For student 11, the standard distance data measured during exercise training by the laboratory is 4,422.15 metres; the motion distance measured by the device in this article is 4,429.15 metres; the motion distance measured by the device in reference 7 is 4,072.70 metres; the motion distance measured by the device in reference 8 is 4,745.39 metres. This article presents a more optimistic view of the reliability of training data compared to standard data, as they enable real-time tracking and documentation of students' exercise training, facilitating better accountability for those records. One area where the device has demonstrated failure is in measuring distance during movement (as shown in student 5). This is an example of where additional engineering is needed to increase stability and optimise the sensors on these devices.

4 Conclusions

Artificial intelligence (AI) continues to have a significant impact on society, and the prevalence of AI-enabled smart wearable technologies is also increasing rapidly. While the growing number of wearable motion-tracking solutions in training has been studied, the application of these devices for training, monitoring, and assessment remains unclear in subsequent research. The theme of this study is the use of wearables as a training tool. The article commences with an overview of the history of research and discusses the

significance of prior research on wearable devices, outlining its benefits and limitations. Following this, device optimisation was performed by developing processes to collect and clean data, and to calibrate the device to establish the validity of the wearable device used in training and its effectiveness in providing training, monitoring, and assessment. According to the current study's findings, heart rate, calories burned, movement speed, and distance moved, as measured by the monitoring device described in this study, are consistent with data collected using standard laboratory procedures. As a result, the device in this study has greater potential than previously believed to be beneficial for monitoring and evaluating training, as well as a strong likelihood of future use.

Although this study has several potential areas for improvement, there are still key considerations. The sample size is limited to undergraduates majoring in physical education. Future researchers should consider including different age groups, genders, and fitness levels to enhance the generalisability of their findings. Another area that needs improvement is the lack of a systematic evaluation of the effects of prolonged device use on battery degradation and sensor drift. Additional research is needed to confirm that this equipment can be relied on over time. Future studies should also assess the interdependencies between the IoT and edge computing, enabling continued validation and optimisation of the equipment over time in real-world settings, where changing conditions create more realistic test conditions.

Declarations

The authors declare that there are no conflicts of interest regarding the publication of this article.

The information of the funding project should be revised as follows: Project Source 1: Hunan International Economics University – Shenzhen Runghoo Technology Co., Ltd. Industry-Education Integration Innovation and Entrepreneurship Education Base (Xiangjiaotong [2022] No. 354).

Project Source 2: Hunan International Economics University – Liuyang Fenghui Ecological Agriculture Co., Ltd. Recreation and Fitness Club Industry-Education Integration Innovation and Entrepreneurship Education Base (Xiangjiaotong [2021] No. 356).

Project Source 3: 2026 University-level Project on Emerging Engineering and Emerging Liberal Arts Research and Practice – 'Construction and practice of the emerging major of sports and senior wellness featuring integration of sports and medicine, industry-education collaboration, and four-dimensional linkage'.

References

Auepanwiriyakul, C., Waibel, S., Songa, J., Bentley, P. and Faisal, A.A. (2020) 'Accuracy and acceptability of wearable motion tracking for inpatient monitoring using smartwatches', *Sensors*, Vol. 20, No. 24, p.7313, https://doi.org/10.3390/s20247313.

Bi, C., Huang, J., Xing, G., Jiang, L., Liu, X. and Chen, M. (2019) 'Safewatch: a wearable hand motion tracking system for improving driving safety', *ACM Transactions on Cyber-Physical Systems*, Vol. 4, No. 1, pp.1–21, https://doi.org/10.1145/3360323.

Birrer, V., Elgendi, M., Lambercy, O. and Menon, C. (2014) 'Evaluating reliability in wearable devices for sleep staging', *NPJ Digital Medicine*, Vol. 7, No. 1, p.74, https://doi.org/10.1038/s41746-024-01016-9.

Dombi, J. and Dineva, A. (2020) 'Adaptive Savitzky-Golay filtering and its applications', *International Journal of Advanced Intelligent Paradigms*, Vol. 16, No. 2, pp.145–156, https://doi.org/10.1504/IJAIP.2020.107011.

Gao, X., Yu, D., Ren, Y., Gao, L. and Xu, L. (2020) 'Delay allocation algorithm for data transmission in wireless sensor networks', *Computer Measurement & Control*, Vol. 28, No. 5, pp.258–262.

Hikmah, I. and Indriyanto, S. (2022) 'Prototype of Body Temperature and Oxygen Saturation monitoring system using DS18B20 and MAX30100 sensors based on IOT', *Jurnal RESTI (Rekayasa Sistem dan Teknologi Informasi)*, Vol. 6, No. 5, pp.810–817, DOI: https://doi.org/10.29207/resti.v6i5.4385.

Hori, K., Uehara, F., Yamaga, Y., Yoshimura, S., Okawa, J., Tanimura, M. et al. (2021) 'Reliability of a novel wearable device to measure chewing frequency', *Journal of Prosthodontic Research*, Vol. 65, No. 3, pp.340–345, https://doi.org/10.2186/jpr.JPR_D_20_00032.

Huang, C-H. and Guo, J-W. (2021) 'Design of reflectance pulse oximeter and bpm using the max30100 sensor in early detection of hypoxemia in patients with cardiovascular disorders', *International Journal of Advanced Health Science and Technology*, Vol. 1, No. 1, pp.1–6.

Jatakar, K.H., Mulgund, G., Patange, A.D., Deshmukh, B.B., Rambhad, K.S., Saxena, A. et al. (2022) 'Vibration monitoring system based on ADXL335 accelerometer and Arduino Mega2560 interface', *Journal of Algebraic Statistics*, Vol. 13, No. 2, pp.2291–2301.

Jiao, M. and Wang, D. (2021) 'The Savitzky-Golay filter-based bidirectional long short-term memory network for SOC estimation', *International Journal of Energy Research*, Vol. 45, No. 13, pp.19467–19480, https://doi.org/10.1002/er.7055.

Kagawade, V.C. and Angadi, S.A. (2021) 'Savitzky-Golay filter energy features-based approach to face recognition using symbolic modeling', *Pattern Analysis and Applications*, Vol. 24, No. 4, pp.1451–1473, https://doi.org/10.1007/s10044-021-00991-z.

Knight, E.C. and Bayne, E.M. (2019) 'Classification threshold and training data affect the quality and utility of focal species data processed with automated audio-recognition software', *Bioacoustics*, Vol. 28, No. 6, pp.539–554, https://doi.org/10.1080/09524622.2018.1503971.

Kuchkorov, A.M.U. (2023) 'Measuring earth's free fall acceleration with ADXL345 accelerometer and Arduino', *Oriental Renaissance: Innovative, Educational, Natural and Social Sciences*, Vol. 3.4, No. 2, pp.589–595.

Kumar, A.S.A., Anandan, N., George, B. and Mukhopadhyay, S.C. (2019) 'Improved capacitive sensor for combined angular and linear displacement sensing', *IEEE Sensors Journal*, Vol. 19, No. 22, pp.10253–10261, DOI: 10.1109/JSEN.2019.2929538.

Liu, S.Q., Zhang, J.C. and Zhu, R. (2019) 'A wearable human motion tracking device using a micro flow sensor incorporating a micro accelerometer', *IEEE Transactions on Biomedical Engineering*, Vol. 67, No. 4, pp.940–948, DOI: 10.1109/TBME.2019.2924689.

Liu, S.Q., Zhang, J.C., Li, G.Z. and Zhu, R. (2020) 'A wearable flow-MIMU device for monitoring human dynamic motion', *IEEE Transactions on Neural Systems and Rehabilitation Engineering*, Vol. 28, No. 3, pp.637–645, DOI: 10.1109/TNSRE.2020.2971762.

Manjarres, J., Narvaez, P., Gasser, K., Percybrooks, W. and Pardo, M. (2019) 'Physical workload tracking using human activity recognition with wearable devices', *Sensors*, Vol. 20, No. 1, p.39, https://doi.org/10.3390/s20010039.

Nickerson, B., Medrano, N.F., Perez, G.L., Narvaez, S.V., Carrillo, J. and Duque, M. (2020) 'Inter-device reliability of wearable technology for quantifying jump height in collegiate athletes', *Biology of Sport*, Vol. 37, No. 4, pp.383–387, DOI: https://doi.org/10.5114/biolsport.2020.96851.

Nimi, W.S., Jose, P.S.H. and Jegan, R. (2021) 'Review on reliable and quality wearable healthcare device (WHD)', *International Journal of Reliable and Quality E-Healthcare (IJRQEH)*, Vol. 10, No. 4, pp.1–25, DOI: 10.4018/IJRQEH.2021100101.

Rahman, M.A., Rashid, M.A. and Ahmad, M. (2019) 'Selecting the optimal conditions of the Savitzky-Golay filter for fNIRS signal', *Biocybernetics and Biomedical Engineering*, Vol. 39, No. 3, pp.624–637, https://doi.org/10.1016/j.bbe.2019.06.004.

Sadeghi, M., Behnia, F. and Amiri, R. (2020) 'Window selection of the Savitzky-Golay filters for signal recovery from noisy measurements', *IEEE Transactions on Instrumentation and Measurement*, Vol. 69, No. 8, pp.5418–5427, DOI: 10.1109/TIM.2020.2966310.

Samann, F. and Schanze, T. (2019) 'An efficient ECG denoising method using discrete wavelet with Savitzky-Golay filter', *Current Directions in Biomedical Engineering*, Vol. 5, No. 1, pp.385–387, https://doi.org/10.1515/cdbme-2019-0097.

Schmid, M., Rath, D. and Diebold, U. (2022) 'Why and how Savitzky-Golay filters should be replaced', *ACS Measurement Science Au*, Vol. 2, No. 2, pp.185–196, https://doi.org/10.1021/acsmeasuresciau.1c00054.

Song, Z., Cao, Z., Li, Z., Wang, J. and Liu, Y. (2021) 'Inertial motion tracking on mobile and wearable devices: recent advancements and challenges', *Tsinghua Science and Technology*, Vol. 26, No. 5, pp.692–705, DOI: 10.26599/TST.2021.9010017.

Su, B., Li, J., Xu, H., Xu, Z., Meng, J., Chen, X. et al. (2022) 'Scientific training assistance: flexible wearable sensor motion monitoring applications', *SCIENTIA SINICA Informationis*, Vol. 52, No. 1, pp.54–74.

Wan, Q., Zhang, Z., Jiang, L., Wang, Z. and Zhou, Y. (2024) 'Image anomaly detection and prediction scheme based on SSA optimized ResNet50-BiGRU model', *Journal of Intelligence Technology and Innovation*, Vol. 2, No. 2, pp.35–52.

Wang, X., Hu, H., Wang, Y. and Wang, Z. (2024) 'IoT real-time production monitoring and automated process transformation in smart manufacturing', *Journal of Organizational and End User Computing*, Vol. 36, No. 1, pp.1–25.

Wilk, M.P., Walsh, M. and O'Flynn, B. (2020) 'Multimodal sensor fusion for low-power wearable human motion tracking systems in sports applications', *IEEE Sensors Journal*, Vol. 21, No. 4, pp.5195–5212, DOI: 10.1109/JSEN.2020.3030779.

Yuan, Z., Zhang, X., Gao, Q., Wang, Z., Cheng, T. and Wang, Z.L. (2022) 'Integrated real-time pneumatic monitoring system with triboelectric linear displacement sensor', *IEEE Transactions on Industrial Electronics*, Vol. 70, No. 6, pp.6435–6441, DOI: 10.1109/TIE.2022.3192690.

Zhang, Y., He, B., Yang, X. and Zhang, W. (2019) 'Overview of human motion tracking methods based on wearable inertial sensors', *Acta Automatica Sinica*, Vol. 45, No. 8, pp.1439–1454, DOI: 10.16383/j.aas.c180367.

Zhang, Z. (2024) 'Deep analysis of time series data for smart grid startup strategies: a transformer-LSTM-PSO model approach', *Journal of Management Science and Operations*, Vol. 2, No. 3, pp.16–43.

Zheng, K. and Li, Z. (2024) 'An image-text matching method for multi-modal robots', *Journal of Organizational and End User Computing*, Vol. 36, No. 1, pp.1–21.

Zhou, H., Lu, T., Liu, Y., Zhang, S. and Gowda, M. (2022) 'Learning on the rings: self-supervised 3d finger motion tracking using wearable sensors', *Proceedings of the ACM on Interactive, Mobile, Wearable and Ubiquitous Technologies*, Vol. 6, No. 2, pp.1–31, https://doi.org/10.1145/3534587.

Zhuo, X., Liu, M., Wei, Y., Yu, G., Qu, F. and Sun, R. (2020) 'AUV-aided energy-efficient data collection in underwater acoustic sensor networks', *IEEE Internet of Things Journal*, Vol. 7, No. 10, pp.10010–10022, DOI: 10.1109/JIOT.2020.2988697.